

## Calibration of an advanced neutral particle analyzer for the Madison Symmetric Torus reversed-field pinch

J. A. Reusch, J. K. Anderson, V. Belykh, S. Eilerman, D. Liu et al.

Citation: *Rev. Sci. Instrum.* **83**, 10D704 (2012); doi: 10.1063/1.4729493

View online: <http://dx.doi.org/10.1063/1.4729493>

View Table of Contents: <http://rsi.aip.org/resource/1/RSINAK/v83/i10>

Published by the [American Institute of Physics](http://www.aip.org).

---

### Additional information on *Rev. Sci. Instrum.*

Journal Homepage: <http://rsi.aip.org>

Journal Information: [http://rsi.aip.org/about/about\\_the\\_journal](http://rsi.aip.org/about/about_the_journal)

Top downloads: [http://rsi.aip.org/features/most\\_downloaded](http://rsi.aip.org/features/most_downloaded)

Information for Authors: <http://rsi.aip.org/authors>

## ADVERTISEMENT

**physicstoday**

Comment on any  
*Physics Today* article.

Physics Today / Volume 63 / Issue 7 / July 2012  
Previous Article | Next Article

**Measured energy in Japan**  
David von Seggern  
(vonseg@seismo.unr.edu) University of Nevada  
July 2012, page 10  
DIGITAL OBJECT IDENTIFIER  
<http://dx.doi.org/10.1063/PT.3.1619>

The article by Thorne Lay and Hiroo Kanamori (2012) is an excellent review of the relationship between seismic moment and energy release. However, they would find that the relationship between seismic moment and energy release is not linear. For a 100-megaton nuclear explosion, the seismic moment is approximately five times as much energy as that of a 100-megaton atmospheric nuclear detonation event—a 40-megaton nuclear device had still more energy by a factor of about 3, or 15 times more energy than that of a 100-megaton atmospheric nuclear detonation event.

The 1964 Chilean earthquake had still more energy by a factor of about 3, or 15 times more energy than that of a 100-megaton atmospheric nuclear device. I believe the authors used the relation for seismic energy release rather than total strain energy release. The seismic energy underestimates the total strain energy release by a variable that depends on the fault plane. Accounting for total strain energy release would increase the earthquake energy number by orders of magnitude.

Despite the catastrophic damage potential of nuclear bombs, the forces of nature occasionally unleash much larger energy releases. Although the nuclear bombs are under our control, earthquakes, volcanic eruptions, and extreme weather events are not. However, by judicious preparation and avoidance measures, humans can significantly diminish the damage of natural events.

The article does not have any references.

**Comment on this article**  
By the act of hitting a ball with a bat, one calculates the force energy to deliver the ball to its new location, but one must also take into account that the ball extended its energy to the strike team, which became struck by the ball as its momentum ceased and passed energy to the strike team. Therefore the parameters of the damage extend into the future when the received energy to that pushed upon, later becomes released in a new event. Perhaps calculations of one added that in, while another's calculations did not. E.M.C.  
Written by Edgar Mocarvill, 14 July 2012 19:59

# Calibration of an advanced neutral particle analyzer for the Madison Symmetric Torus reversed-field pinch<sup>a)</sup>

J. A. Reusch,<sup>1,b)</sup> J. K. Anderson,<sup>1</sup> V. Belykh,<sup>2</sup> S. Eilerman,<sup>1</sup> D. Liu,<sup>3</sup> G. Fiksel,<sup>4</sup> and S. Polosatkin<sup>2</sup>

<sup>1</sup>University of Wisconsin-Madison, Madison, Wisconsin 53706, USA

<sup>2</sup>Budker Institute of Nuclear Physics SB RAS, Novosibirsk, Russia

<sup>3</sup>University of California-Irvine, Irvine, California 92697, USA

<sup>4</sup>University of Rochester, Rochester, New York 14623, USA

(Presented 9 May 2012; received 7 May 2012; accepted 25 May 2012; published online 25 June 2012)

A new  $\mathbf{E}\parallel\mathbf{B}$  neutral particle analyzer, which has recently been installed on Madison Symmetric Torus (MST) reversed-field pinch (RFP), has now been calibrated, allowing the measurement of the fast ion density and energy distribution. This diagnostic, dubbed the advanced neutral particle analyzer (ANPA), can simultaneously produce time resolved measurements of the efflux of both hydrogen and deuterium ions from the plasma over a 35 keV energy range with an energy resolution of 2–4 keV and a time resolution of 10  $\mu\text{s}$ . These capabilities are needed to measure both majority ion heating that occurs during magnetic reconnection events in MST and the behavior of the fast ions from the 1 MW hydrogen neutral beam injector on MST. Calibration of the ANPA was performed using a custom ion source that resides in the flight tube between the MST and the ANPA. In this work, the ANPA will be described, the calibration procedure and results will be discussed, and initial measurements of the time evolution of 25 keV neutral beam injection-born fast ions will be presented. © 2012 American Institute of Physics. [<http://dx.doi.org/10.1063/1.4729493>]

## I. INTRODUCTION

The recent addition of a 1 MW, tangential neutral beam injector<sup>1,2</sup> on the Madison Symmetric Torus (MST)<sup>3</sup> has facilitated the study of fast ion dynamics and momentum transport in the reversed-field pinch (RFP). While acceleration of thermal ions and the generation of non-Maxwellian ion distributions during magnetic reconnection events have been studied in the RFP in the past, it is only now, with the installation of high power neutral beams on multiple RFPs, that the behavior of fast beam-born ions can be investigated in the RFP configuration. To that end, the advanced neutral particle analyzer (ANPA) has been added to the diagnostic set of MST. This diagnostic is capable of simultaneously measuring hydrogen and deuterium fast neutrals with energies up to 45 keV and an energy range of 35 keV. The flexible design of the ANPA also allows this 35 keV energy range to be shifted down in order to detect thermal neutrals and the 25 keV beam neutrals at the same time. This diagnostic greatly enhances our ability to measure the time evolution of both the beam-generated fast hydrogen distribution and a fast deuterium population that is generated during global reconnection events that occur in standard MST discharges. While there is a great deal of physics that can, and soon will, be studied with this diagnostic, this work focuses on the calibration of the diagnostic, which is critical to gaining a quantitative understanding of the fast ion population in MST.

## II. HARDWARE

Designed at the Budker Institute of Nuclear Physics (BINP) in Russia, details of the ANPA design have appeared elsewhere,<sup>4,5</sup> but specifics of the device implemented on MST will be presented here. The ANPA is compact, measuring just 28 cm across, which allows the diagnostic to be moved with relative ease between radial and tangential views. This is significant as it makes it possible to measure both the parallel and perpendicular components of the distribution function with a single diagnostic. The ANPA, shown in Fig. 1, consists of five primary components: the electron stripping foil, the electrostatic focusing lens, the magnet for energy separation, the capacitor for mass separation, and the secondary electron multipliers (SEMs) used to detect the incident ions at 10 locations for each species (for a total of 20 channels). The vacuum housing, lens, capacitor, and 0.6 T magnet were provided by BINP. The stripping foil is made by the Lebow company and consists of a 10 nm thick carbon foil on a Ni mesh support. The foil is mounted on an Al ring with a 5 mm inner diameter which provides the limiting aperture for the field of view of the diagnostic. The SEMs selected for this diagnostic are the MAGNUM 5900 from Photonis. The stripping foil bias, SEM bias, lens, and capacitor voltages are provided by high voltage power supplies from UltraVolt Inc. All of the high voltage supplies are controlled over ethernet via the analogue output of a pocket PLC (Galil RIO-47100).

In addition to the ANPA itself, the BINP design includes an integrated ion source for *in situ* calibration (see Fig. 1). The operating principle of the ion source is similar to the Bayard-Alpert high vacuum gauge. The source consists of a thoriated tungsten filament that is biased  $-200$  V with respect to a

<sup>a)</sup>Contributed paper, published as part of the Proceedings of the 19th Topical Conference on High-Temperature Plasma Diagnostics, Monterey, California, May 2012.

<sup>b)</sup>Author to whom correspondence should be addressed. Electronic mail: jareusch@wisc.edu.

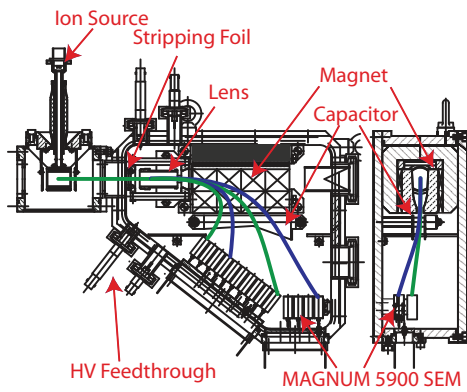


FIG. 1. This figure shows a schematic view of the major components of the ANPA including the ion source. MST is off the figure to the left. The green lines show the hydrogen trajectories while the blue show the deuterium trajectories for the lowest and highest energy channels.

can shaped cylindrical mesh that is held at high potential with respect to a set of grounded grids about 1 cm from the ends of the mesh can. The mesh can and the grounded grids are nearly transparent to neutrals and so the entire apparatus resides in the beam line during operation. The energy of the ions produced by the source is fundamentally limited by the three conductor vacuum feedthrough, but in practice is limited by the high voltage bias supply (UltraVolt 40A-12-P4-C) at 43 kV.

### III. CALIBRATION

The ion source provides a straightforward way to calibrate the ANPA. The energy calibration can be done in place by continuously scanning the voltage on the ion source from 43 kV to 0 V. Performing an absolute calibration is somewhat more involved as the total number of each species of ion incident on the foil must be known as well. To this end, the absolute calibration of the ANPA was performed on the bench with a faraday cup (Beam Imaging Solutions model FC-1) placed on what is normally the MST side of the ion source (see Fig. 2). The faraday cup is biased to +18 V in order to avoid secondary emission current. Since the source design is symmetric, the current output from the SEMs for each of the 10 hydrogen detectors is compared to the total current measured by the faraday cup. In practice, the source is not perfectly symmetric, but the output from one side is generally proportional to the other and has been accounted for in the following analysis.

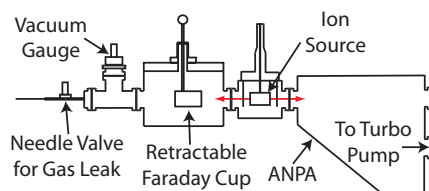


FIG. 2. Schematic view of the calibration setup. A gas bottle attached to the needle valve on the left side can provide a controlled leak of a particular gas if desired. The faraday cup is retractable for possible *in situ* absolute calibration in the future.

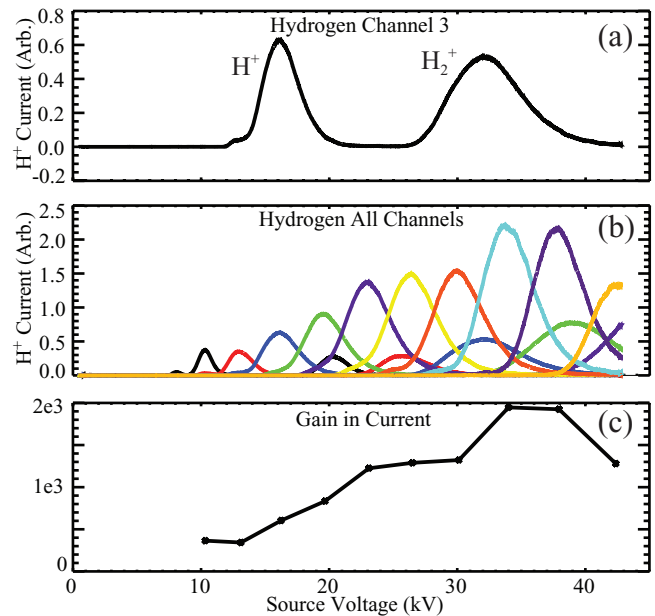


FIG. 3. Panel (a) shows one of the lower energy channels in which the  $H^+$  and  $H_2^+$  peaks can be seen clearly. Panel (b) shows all 10 of the hydrogen channels. Panel (c) shows the absolute gain in current of the ANPA.

In order to perform the absolute calibration of the hydrogen channels, which will only detect  $H^+$  ions, with the faraday cup, which will measure the total incident ion current, the relative contribution of each species of ion generated by the ion source must be determined. The  $H^+$  ions were generated by electron impact ionization of the residual water vapor in the ion source. This process generates two products that can be measured by the ANPA,  $H^+$  and  $H_2^+$ . It is assumed that these ions dominate the faraday cup signal; however, work is ongoing to properly quantify the contributions from heavier ions such as  $H_2O^+$  and  $OH^+$ . Sweeping the voltage over the full range of the source shows two clear peaks in each of the lower energy hydrogen channels (see Fig. 3(a)). The first peak is due to  $H^+$  ions which have passed through the stripping foil and continued to the detectors. The second is due to  $H_2^+$  molecular ions which split upon hitting the foil to become a pair of hydrogen ions moving at half the velocity of the primary hydrogen ions. It should be noted that there is also a small contribution from hydrogen ions that neutralize ( $H_0$ ) before they reach the stripping foil and are then ionized. The three species can be easily distinguished by biasing the stripping foil with respect to ground. The  $H^+$  ions decelerate towards and accelerate away from the foil in equal amounts, and thus the central energy for this peak will not change with changing foil bias. The  $H_2^+$  signal will shift towards the  $H^+$  peak with increasing foil bias as they will see twice as much acceleration as deceleration. The  $H_0$  peak will shift to lower energy, away from the  $H^+$  peak, as it will see no deceleration and the full acceleration due to the foil bias. For this setup used here, the  $H_0$  contribution is negligible.

The relative contribution of the  $H_2^+$  and  $H^+$  species to the faraday cup current is determined by comparing the relative heights of their respective peaks seen in the SEM signals during a voltage sweep. The  $H_2^+$  peak is generally about 25%

smaller than the  $H^+$  peak and the SEM will register twice as much current from the  $H_2^+$  than the faraday cup will because the SEM registers two  $H^+$  ions for each  $H_2^+$ . Given this information, the  $H^+$  current is found to be roughly 72% of the current measured by the faraday cup. Combining this information with the differences in area of the stripping foil and the faraday cup as well as the asymmetry of the ion source, the absolute gain for each channel can be determined. Figure 3(b) shows the calibration scan for the full set of 10 hydrogen channels. While the peaks are distinct, there is significant channel to channel overlap indicating that the ion beam, after passing through the carbon foil, is poorly focused. Work is ongoing to optimize the focusing optics to minimize this overlap. Figure 3(c) shows the gain coefficients relating the SEM current output to the current incident on the stripping foil.

While ionization of residual gas works well for the relative calibration of the hydrogen channels, it does not work for calibration of the deuterium channels as there is very little residual deuterium in the diagnostic. For calibrating the deuterium channels, a  $2 \times 10^{-5}$  torr deuterium leak was supplied through the needle valve shown on the left side of Fig. 2 (the nominal base pressure was  $2 \times 10^{-6}$  torr). However, electron impact ionization of  $D_2$  preferentially generates  $D_2^+$ , and thus the much smaller  $D^+$  signal was nearly washed out. An alternate approach is to use a fill gas that does not produce as much molecular deuterium. Deuterated methane, which is available from Cambridge Isotope, is one such molecule and will be pursued in the near future. Despite this difficulty, an initial relative calibration of the deuterium channels has been performed by identifying and fitting the  $D^+$  peak for each channel.

#### IV. INITIAL DATA

This diagnostic has now been used on MST to measure two different components of the fast ion distribution. The first is a radial view which is primarily sensitive to fast ions with high  $v_{\perp}$ . The second is a toroidal view which measures fast ions from the core with high  $v_{\parallel}$  and in the edge with high  $v_{\perp}$ . A more detailed discussion of this analysis can be found in S. Eilerman *et al.*<sup>6</sup> Figure 4 shows ANPA data from a standard MST discharge taken on the tangential view. The fast ion distribution is very dynamic in time with clear indications of ion acceleration at sawteeth. After the beam turns off, the signal decays in a way that is consistent with classical slowing of the fast ions, suggesting that the fast ions are well confined in MST plasmas.

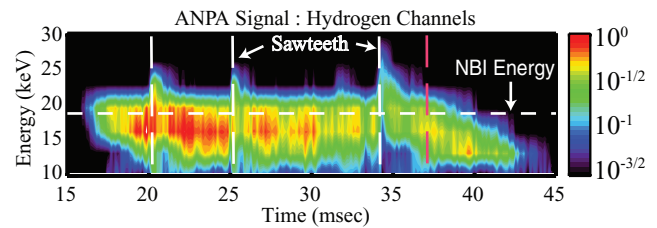


FIG. 4. ANPA data from neutral beam injection (NBI) into a standard MST discharge. The NBI turns on at 15 ms and turns off at 37 ms (red dashed line). The beam, run at 19 keV for this experiment, is clearly visible as is the fast ion acceleration at sawtooth events.

#### V. CONCLUSIONS

The addition of the ANPA to the diagnostic set on MST has greatly enhanced our ability to understand the time dynamics of fast ions traveling both parallel and perpendicular to the magnetic field. Absolute calibration of this diagnostic not only allows the characterization of the shape of the fast ion distribution, but also the fast ion density. This makes it possible to study fast ion confinement and  $\beta$  values (which TRANSP modeling suggests may be as high as 10%) as well as acceleration and heating mechanisms believed to be active during global magnetic reconnection events that occur in standard discharges in MST.<sup>7</sup>

#### ACKNOWLEDGMENTS

This work was done under the financial support of the (U. S.) Department of Energy (DOE) and the Russian Ministry of Science and Education.

- <sup>1</sup>J. Anderson, A. Almagri, B. Chapman, V. Davydenko, P. Deichuli, D. Den Hartog, C. Forest, G. Fiksel, A. Ivanov, D. Liu, M. Nornberg, J. Sarff, N. Stupishin, and J. Waksman, *Trans. Fusion Sci. Technol.* **59**, 27 (2011).
- <sup>2</sup>D. Liu, A. F. Almagri, J. K. Anderson, V. V. Belykh, B. E. Chapman, V. I. Davydenko, P. Deichuli, D. J. D. Hartog, S. Eilerman, G. Fiksel, C. B. Forest, A. A. Ivanov, J. Koliner, M. D. Nornberg, S. V. Polosatkin, J. S. Sarff, N. Stupishin, and J. Waksman, in *12th IAEA Technical Meeting on Energetic Particles in Magnetic Confinement Systems* (Austin, Texas, 2011), pp. 1–8.
- <sup>3</sup>R. Dexter, D. Kerst, T. Lovell, and S. Prager, *Fusion Sci. Technol.* **19**, 131 (1991).
- <sup>4</sup>S. Polosatkin, *Fusion Sci. Technol.* **59**, 259 (2011).
- <sup>5</sup>S. Polosatkin, V. Belykh, V. Davydenko, R. Clary, G. Fiksel, A. Ivanov, and V. Kapitonov, “Neutral particle analyzer for studies of fast ion population in plasma,” *Nucl. Instrum. Methods Phys. Res. A* (to be published).
- <sup>6</sup>S. Eilerman, J. K. Anderson, J. A. Reusch, D. Liu, G. Fiksel, S. Polosatkin, and V. Belykh, “Time-resolved ion energy distribution measurements using an advanced neutral particle analyzer on the MST reversed-field pinch,” *Rev. Sci. Instrum.* (these proceedings).
- <sup>7</sup>R. Magee, D. Den Hartog, S. Kumar, A. F. Almagri, B. Chapman, G. Fiksel, V. Mironov, E. Mezonlin, and J. Titus, *Phys. Rev. Lett.* **107**, 065005 (2011).